

NASA Technical Memorandum 103645  
AIAA-90-3953

# Near-Field Noise of a Single-Rotation Propfan at an Angle of Attack

M. Nallasamy and E. Envia  
*Sverdrup Technology, Inc.*  
*Lewis Research Center Group*  
*Brook Park, Ohio*

and

B.J. Clark and J.F. Groeneweg  
*National Aeronautics and Space Administration*  
*Lewis Research Center*  
*Cleveland, Ohio*

Prepared for the  
13th Aeroacoustics Conference  
sponsored by the American Institute of Aeronautics and Astronautics  
Tallahassee, Florida, October 22-24, 1990



(NASA-TM-103645) NEAR-FIELD NOISE OF A  
SINGLE-ROTATION PROPFAN AT AN ANGLE OF  
ATTACK (NASA) 20 p CSCL 20A

N91-12316

Unclas

G3/71 0312064



# Near-Field Noise of a Single-Rotation Propfan at an Angle of Attack

M. Nallasamy and E. Envia  
Sverdrup Technology, Inc.  
Lewis Research Center Group  
Brook Park, Ohio

and

B. J. Clark and J. F. Groeneweg  
NASA Lewis Research Center  
Cleveland, Ohio

## Summary

The near-field noise characteristics of a propfan operating at an angle of attack are examined utilizing the unsteady pressure field obtained from a three-dimensional Euler simulation of the propfan flowfield. The near-field noise is calculated employing three different procedures: a direct computation method in which the noise field is extracted directly from the Euler solution, and two acoustic-analogy-based frequency domain methods which utilize the computed unsteady pressure distribution on the propfan blades as the source term. The inflow angles considered are -0.4, 1.6, and 4.6 degrees. The results of the direct computation method and one of the frequency domain methods show qualitative agreement with measurements. They show that an increase in the inflow angle is accompanied by an increase in the sound pressure level at the outboard wing boom locations and a decrease in the sound pressure level at the (inboard) fuselage locations. The trends in the computed azimuthal directivities of the noise field also conform to the measured and expected results.

## Introduction

The advanced propfan program initiated by NASA in the mid-seventies culminated in flight test/demonstration of single and counter-rotation propfan systems[1]. The NASA Lewis advanced turboprop project included wind tunnel tests of a series of propfan models, and wind tunnel and flight tests of a large-scale propfan system. A large-scale 9-foot (2.74m) diameter, NASA-Hamilton Standard single rotation eight bladed tractor configuration was flight tested in 1987-88. The propfan was mounted on the left wing of an instrumented Gulfstream II testbed aircraft, modified for the propfan tests (Fig. 1a). The Propfan Test Assessment program (PTA) was conducted by Lockheed Aeronautical Systems Company for NASA Lewis Research Center. The overall

objectives of the PTA program were to evaluate the propfan structural integrity, source noise, cabin noise, and enroute noise[2,3].

In the PTA program, a nacelle tilt arrangement was employed to vary the inflow angle to the propfan. The nacelle tilt angles considered were -3, -1 (tilt down) and +2 (tilt up) degrees. The average inflow angle to the propfan, however, is dependent not only on the nacelle tilt angle but also on the airplane angle of attack and the upwash angle at the propfan (Fig. 1b). For the cruise operating conditions of interest here the airplane mean angle of attack was 1.6 degrees. The upwash angle at the propfan estimated from panel method calculations[3] was about 1.0 degree. Thus, the estimated propfan inflow angles[4] corresponding to the nacelle tilt angles of -3, -1 and +2 degrees were -0.4, 1.6 and 4.6 degrees, respectively.

The variations in inflow conditions were used to evaluate the effects of cyclic stresses on the propfan performance over a wide range of operating conditions. In particular, the effects of inflow conditions on the near-field noise characteristics were studied for takeoff and cruise operating conditions. In this paper attention is restricted to the near-field noise characteristics at cruise conditions. The measurements show that an increase in inflow angle is accompanied by an increase in sound pressure level (SPL) at the wing boom and a simultaneous decrease in SPL at the fuselage[4]. In the PTA tests and predictions reported in this paper, the sense of rotation of the propfan is inboard up.

The prediction of the effect of inflow angle on the near-field SPL characteristics requires knowledge of the unsteady flowfield of the propfan. The numerical solution of the three-dimensional Euler equations governing the flowfield offers an enticing possibility. Nallasamy and Groeneweg[5] reported unsteady Eu-

ler solutions of the flowfield of a propfan at angle of attack for three inflow angles of  $-0.4$ ,  $1.6$  and  $4.6$  degrees. The conditions chosen for that study correspond to the PTA flight test cruise conditions with a blade tangential tip speed of  $797$  ft/sec ( $243$  m/sec). The computed unsteady blade surface pressure distributions were compared with wind tunnel data[6,7] and found to be in reasonable agreement.

In the present investigation, the near-field noise characteristics are examined as a function of inflow angle employing the unsteady flowfield solutions of Nallasamy and Groeneweg[5]. The near-field SPLs are computed using three different methods to be described later. The computed SPLs are compared with the PTA measurements.

### Unsteady flowfield solutions

The unsteady three-dimensional Euler solutions reported in reference 5 are used for the present near-field acoustic calculations. The salient features of the unsteady solutions are briefly described here for clarity and aid in understanding of the acoustic calculations. Fig. 2 shows the computed azimuthal variations of blade loading due to angular inflow for three inflow angles,  $-0.4$ ,  $1.6$  and  $4.6$  degrees. The azimuth angle is measured from the vertical(top-dead-center, Fig. 1c). The sinusoidal variation of the integrated blade loading due to angular inflow is evident. A substantial variation of the loading( $\pm 81\%$ ) about the mean is observed for  $4.6$  degrees inflow angle. The variations of the integrated blade loading with inflow angle is shown in Fig. 3 for two azimuthal locations  $\phi = 90$  degrees (boom side), and  $\phi = 270$  degrees (fuselage side). An increase in the inflow angle causes the blade loading on the boom side to increase, but that on the fuselage side to decrease.

The variation of elemental power coefficient with inflow angle for four azimuthal positions,  $\phi = 0$ ,  $90$ ,  $180$ , and  $270$  degrees is shown in Fig. 4. At  $\phi = 0$  and  $270$  degrees locations the blade loading decreases with increase in the inflow angle throughout the blade span. The blade loading increases with increase in the inflow angle over the entire span at  $\phi = 90$  and  $180$  degrees locations.

Typical azimuthal variations (waveforms) of unsteady pressure coefficients are shown in Fig. 5. The figure shows the waveforms at the 75% radial station at three normalized chordwise locations,  $0.1$ ,  $0.5$  and  $0.9$ , on the suction and pressure sides of the blade. The blade response increases with inflow angle as would be expected. Non-sinusoidal responses are observed for  $4.6$  degrees inflow angle both on the suction and pressure sides due to the presence of shock

waves[5]. The variation of blade response with axial distance (chord) is also illustrated. These blade surface pressure distributions form the input for the two frequency-domain acoustic calculations described later. Further details of the azimuthal, chordwise, and spanwise variations of the blade surface pressures and blade loading may be found in[4].

### Near-field Acoustic Calculations

The noise levels at the microphone locations on the boom and fuselage sidelines, at a distance of  $1.12D$  ( $D$  is the propfan diameter) from the axis, were computed for comparisons with measured values. The azimuthal and axial locations of the boom microphones and fuselage microphones opposite the boom are shown in Figs. 6a and 6b, respectively. Note that the geometric observation angle at any microphone changes with the nacelle tilt since the propfan center moves up or down relative to the fixed boom and fuselage microphones(Fig. 6a).

The noise predictions were obtained employing three methods: a direct numerical computational procedure and two frequency domain analysis methods. A brief description of each of these methods is given below.

#### (i) Direct numerical computation procedure (DCP)

In this method the propfan near-field noise is extracted from the pressure field obtained from solving the three-dimensional Euler equations. For a steady flow(i.e., zero inflow angle) since the flowfield in each blade passage is identical, the Euler solution is usually carried out for only one blade passage. From such an Euler solution, a spatial pressure distribution in the azimuthal(blade to blade) direction is obtained for a specified observer location. The spatial pressure pattern is transformed into the time domain using the rotational speed and blade count of the propeller. Finally, the pressure-time history thus obtained is Fourier analyzed for its spectral content.

Since in the DCP method the acoustic pressure is extracted directly from the field pressure, it includes the nonlinear propagation effects which are not typically accounted for in conventional methods based on acoustic analogy. The DCP method, however, suffers from the limitations of the flowfield resolution in the regions away from the propfan blade. This procedure(DCP) was previously employed for steady flow (i.e., zero inflow angle) conditions by Korkan et al.[8] and Whitfield et al.[9]. Their Euler solution suffered from low grid resolution in regions away from the blade due to grid clustering schemes typically employed in these computations. Hence, Whitfield et al.

computed the sound pressure levels using DCP at distances close to the blade and then extrapolated their results to the observer(microphone) locations of interest.

In contrast to the zero inflow angle case described above, for a propeller operating at an angle of attack, the unsteady Euler equations must be solved for the entire flowfield (i.e., all blade passages). The flowfield in each passage is different due to variations in local flow incidence angles as a result of the angular inflow. Also, in this case the pressure-time history at any observer position can be obtained directly from the unsteady three-dimensional Euler solution. The pressure waveform is obtained by storing the pressure computed at an observer location as the blades rotate past it as is done in a physical experiment. But no ensemble averaging is done in the computations! The harmonic content is then extracted as in the steady case by a Fourier representation of the pressure waveform.

In the unsteady Euler computations of PTA cruise test cases for the three inflow angles, a grid distribution of the type shown in Fig. 7 was employed. This figure shows the axial-radial surface grid. The waveforms extracted at the PTA sideline microphone location(1.12D) indicated that the flow resolution there is not sufficient for such purposes. Hence, following the procedure of Whitfield et al.[9], as a first approximation, the acoustic pressure waveforms are computed at a radial location of 0.53D from the propfan axis. The observer angles/axial locations of the PTA microphones and the locations selected for computation are shown in Fig. 7. The computed results are then extrapolated to the actual PTA microphone sideline distance(1.12D) using a simple inverse square distance law.

Unlike the DCP method described above, the frequency domain methods utilize the concept of acoustic analogy to estimate the acoustic radiation from rotating propellers. In these methods the propfan blade unsteady surface pressure distributions are used as source strengths which then replace the propfan altogether.

#### (ii) Hansons's Frequency-Domain Theory (FDH)

This theory known as the helicoidal surface theory, was developed by Hanson[10]. It is widely used for propfan noise studies. It employs the helicoidal surface representation of the moving sources to derive a near/far field estimate of the noise radiation from propfans. Based on this theory and its companion aerodynamic theory[11] a computer program called

Unified Aero-Acoustic Program (UAAP) was developed by Hamilton Standard for NASA Lewis. In the present study the acoustics part of UAAP was used to compute the near-field noise for the PTA angular inflow cases. The azimuthal variation of blade loading (waveform) obtained from the Euler solution is represented by a Fourier series and the unsteady loading harmonics are used as input to the UAAP. The UAAP computes the SPLs, taking one blade loading order (harmonic) input at a time. Once noise levels from all loading orders of interest are computed, they are added together accounting for their proper phases. The SPLs reported here are the ones computed for the first three unsteady blade loading orders.

#### (iii) Frequency Domain Formulation of Envia (FDE)

This method uses a version of the Ffowcs Williams-Hawkings[12] equation derived for a uniformly moving medium. This formulation is a natural choice for comparisons with the PTA inflight measurements as well as wind tunnel data. Like the FDH method, FDE method is carried out in the frequency domain but unlike the former, it does not rely on the near/far approximations of a certain integral. In the FDE method this integral is evaluated utilizing an efficient numerical integration scheme(Romberg integration). The use of a simple numerical integration scheme further affords the flexibility of using a source strength that can have an arbitrarily complex time-dependent behavior without the need to decompose the source strength time history into its constituent Fourier components. Furthermore, the use of the numerical integration allows the inclusion of the cross-flow convective phase effects (i.e., Mani's "added phases"[13]) which are present whenever the inflow angle into the propeller is non-zero. In fact, in the FDE method, this effect is accounted for in an exact manner for arbitrarily large cross-flow components. The contribution due to Mani's added phases to the computed SPL is, however, small for the inflow angles and cruise operating conditions considered here.

In addition to the above issue, there is another important difference between the FDH and FDE methods. In the FDH method, the local integrated "pressure force" (i.e., lift) is taken to be perpendicular to the local direction of motion rather than the local blade surface. This "2-D" description of loading impacts the acoustic predictions in two ways. Firstly, since it basically excludes any radial loading contribution it does not account for the effect of the radial dipole which cannot be neglected in the vicinity of the plane of rotation of the propeller. Secondly, by

placing the sectional lift perpendicular to the local direction of motion, all of the local acoustic dipoles at a given radial station are, in effect, aligned with each other. This, in turn, tends to reduce the mutual interference between them which otherwise might exist. By placing the local loading perpendicular to the local blade surface, as is done in the FDE method, a more realistic distribution for the acoustic sources is obtained. It should be mentioned that the effects alluded to here tend to be unimportant for the conventional straight blade propellers of the type used in general aviation. Details of the FDE formulation may be found in[14].

### Results and Discussion

The near-field noise levels of the propfan operating at angle of attack have been computed for the PTA cruise test conditions. The propfan inflow angles considered are -0.4, 1.6, and 4.6 degrees. The cruise test conditions are: Mach number = 0.8, advance ratio = 3.12, altitude = 35000 ft (10,670 m) and blade tangential tip speed = 797 ft/sec (243 m/sec). The near-field noise levels computed by the three methods described above are compared with the PTA measurements.

The wing acoustic boom on the PTA tapers from 6-1/4 in. (15.8 cm) diameter at the microphone at 1.0D (closest to the wing) to 1-5/8 in. (4.1cm) diameter at -0.5D (forward) microphone. The scattering from the boom affects the SPLs measured at the boom microphones. The boom scattering at the microphone locations computed using reference 15 was reported by Dittmar[16]. The pressure amplifications for the boom microphones going from forward to aft are 0, 0.5, 0.5, 1.0 and 1.5 dB for the blade passing frequency (BPF) tone; 0.5, 1.5, 1.5, 2.0, and 2.5 dB for 2BPF; and 1.0, 2.0, 2.5, 3.5, and 4 dB for 3BPF. These boom amplifications are subtracted from the measured boom tones (Figs. 8, 10 and 11) for comparisons with the computed results. The fuselage is assumed to have a 6dB pressure amplification and this value is subtracted from the fuselage data (Fig. 9) for comparison with predictions.

Figure 8 shows the effect of inflow angle on the area-maximum SPL at the blade passing frequency at the outboard wing boom microphone side-line. The area-maximum SPL here is the maximum of the SPLs recorded at five boom microphone locations (see Fig. 6b for microphone locations). At these locations, measurements (Fig.8) show that an increase in inflow angle increases the fundamental tone SPL. The SPLs computed by the DCP and FDE methods show

the same trend. On the boom side, the SPL increases with increase in inflow angle as does the blade loading (Fig.3). The results of the FDH method show little sensitivity to the inflow angle. Such an insensitivity in the predictions from the FDH method was also reported in[17] (see also[4]). It should be noted that the predictions reported in[17] were obtained using a different unsteady blade loading distribution. In view of the discussion in the previous section concerning the differences between the FDH and FDE methods, perhaps the apparent insensitivity of the FDH predictions to the inflow angle changes is related to the manner in which the loading dipoles are implemented in that method.

Figure 9 shows the effect of inflow angle on the area-maximum SPL at the BPF at the inboard fuselage microphone sideline. The area-maximum SPL here refers to the maximum of the SPLs recorded at the eight fuselage microphone locations (Fig. 6b shows these microphone locations). On the fuselage side (Fig. 9), the measurements show that an increase in inflow angle causes a decrease in fundamental tone SPL. The results of DCP and FDE calculations show a similar trend. However, in the computations the slope of the line is steeper than in the measurements. On the fuselage side, the SPL decreases with increases in inflow angle as does the blade loading (see Fig. 3). Again, the results from the FDH method show little sensitivity to inflow angle changes. It should be noted that the computed results shown in Fig. 9 are free field and do not include corrections for boundary layer refraction and wing reflection effects. Since no model for these effects has been included in the present computations further comparisons with data will be limited to boom microphone locations.

The predicted sensitivities of the first, second and third harmonic SPLs to inflow angle by the three methods at the boom microphone locations are compared with measurements in Figs. 10a - 10e. The fundamental tones measured at all the five boom microphone locations generally show an increase with inflow angle. This trend is well represented by the two predictions, DCP and FDE. The computed absolute magnitudes, however, show a mixture of under- and over-prediction. The DCP computations depend on the flow field resolution at the computational points. Since the location of the forward microphone at -0.5D is in the region of poor flow field resolution, no results of DCP for this location are presented here and in Fig. 11. The FDH calculations show a marginal increase of SPL with inflow angle at the two microphones located far aft (1.0D) and forward (-0.5D). The measurements may have been influenced by scattering at

the boom surface and reflections from the wing both of which depend on the microphone location. The measurements have been corrected only for the boom scattering effects as mentioned above.

The SPL measurements of the second and third harmonics at the boom microphone locations do not show a consistent trend with inflow angle. The computations of FDE and DCP show an increase in SPL with increase in inflow angle. The results of the DCP method, in general, produce levels of higher harmonics much lower than the measured ones.

The sideline BPF tone SPL directivities of the boom microphones for the three inflow angles, -0.4, 1.6, and 4.6 degrees are shown in Figs. 11a, 11b and 11c, respectively. In each of the figures, the measured maximum SPL occurs at the microphone located 0.25D aft of the plane of rotation (POR). The predictions from the DCP and FDE methods also show that, in each case, the maximum level occurs at the same location. The FDH predictions, however, show the maximum level in each case to occur in the plane of the propfan.

Fig. 12 shows the measured and computed sound pressure time histories for the boom microphone located at 0.25D aft of the POR for an inflow angle of 1.6 degrees. The peak levels computed by FDE are higher than those of the DCP predictions and the PTA data as implied by the dB levels in Figs. 8-11. The computed sound pressure waveforms are similar to but differ from the measured one in that the existence of a 'zone' of near-zero pressure amplitude (for about 30% of a period) between positive and negative peaks in the measurements is not predicted.

An interesting near-field noise characteristic of a propfan operating at angle of attack is the effect of inflow angle on the azimuthal directivity. The azimuthal directivities computed by FDE and DCP methods are shown in Figs. 13a and 13b respectively. In both figures, fuselage side ( $\phi = 270$  degrees) and above the propfan ( $\phi = 0$  degree) locations show a decrease in fundamental tone SPL with increase in the inflow angle. This is consistent with the blade elemental power coefficient variations in Fig. 4, which also show a decrease in blade power with increases in inflow angle for  $\phi = 0$  and 270 degrees. On the other hand, the boom side ( $\phi = 90$  degrees) and below the propfan ( $\phi = 180$  degrees) locations show an increase in fundamental tone SPL with increase in the inflow angle. This again is consistent with the blade power variations in Fig. 4, which show that for  $\phi = 90$  and 180 degrees, blade power increases with

increases in inflow angle. There exist two small azimuthal regions about  $\phi = 45$  degree and  $\phi = 225$  degree where the inflow angle variations have little effect on the computed fundamental tone SPLs. The azimuthal directivity is also consistent with the notion that with angular inflow (as in takeoff cases) the noise level above the propfan decreases and that below the propfan (on the ground) the noise level increases [18,19]. The minimum noise level predicted by the DCP method is much lower than that computed with the FDE method.

Fig. 14 shows the sideline BPF tone directivities computed as a continuous function of axial distance with the FDE method for boom and fuselage locations opposite the boom. On the boom side (Fig. 14a), an increase in inflow angle increases the fundamental tone SPL over the entire axial distance, -0.5D to 1.0D aft of the POR. However, on the fuselage side (Fig. 14b), an increase in inflow angle decreases the fundamental tone SPL only in the range of axial distance 0.0 to 1.0D. At locations ahead of the POR and beyond 1.0D aft of it no clear trend is observed. In this range, an inflow angle of 4.6 degrees produces levels of SPL higher than those for the other two inflow angles. Note that the plot shows only the results of the free field computation.

### Concluding Remarks

The effect of inflow angle on the near-field noise of a propfan operating at cruise conditions has been studied using a direct computation procedure and two frequency domain methods. All three acoustic calculations use the same unsteady blade pressure, loading and flow field information from an unsteady three-dimensional Euler solution. The results of the DCP and FDE methods are in qualitative agreement with measurements. The computed SPLs at the wing boom locations increase with angle of attack whereas those on the fuselage locations opposite the boom decrease with increasing inflow angle for an inboard-up propfan rotation. Models for the fuselage boundary layer refraction, reflections from the wing surface etc. need to be included for more meaningful comparisons of the computed absolute levels with measurements.

The direct numerical computation of the noise levels from the Euler solution appears to be a useful near-field analysis technique. However, the accuracy of the direct computation depends on the flowfield resolution at the observer position. Advances in computational fluid dynamics algorithms and availability of supercomputer time and memory are expected to make the required field resolution possible. Then,

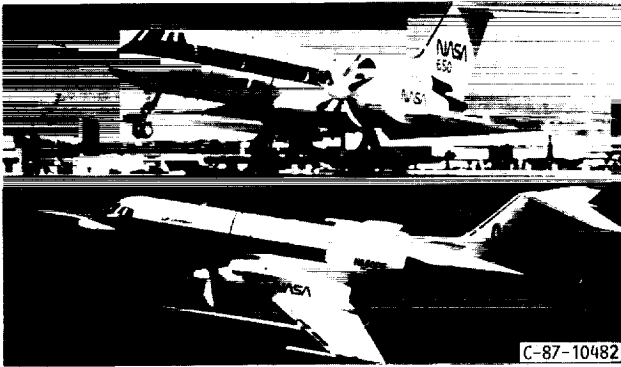
the direct computation procedure may become a viable and reliable method of computing near-field noise characteristics of a propfan.

#### REFERENCES

1. Hager, R.D and Vrabel, D., "Advanced Turboprop Project," NASA SP-495, 1988.
2. Poland, D.T., Bartel, H.L., and Brown, P.C., "PTA Flight Test Overview," AIAA paper 88-2803, July 1988.
3. Little, B.H., Bartel, H.N., Reddy, N.N., Swift, G., and Withers., "Propfan Test Assessment (PTA) Flight Test Report," NASA-CR-182278, April 1989.
4. Bartel, H.W. and Swift, G., "Near-Field Acoustic Characteristics of a Single-Rotation Propfan," AIAA paper 89-1055, April 1989.
5. Nallasamy, M and Groeneweg, J.F., "Unsteady Euler Analysis of the Flow Field of a Propfan at an Angle of Attack," AIAA Paper 90-0339, Jan. 1990.
6. Heidelberg, L.J., and Nallasamy, M., "Unsteady Blade Surface Measurements for the SR7-A Propeller at Cruise Conditions," AIAA Paper 90-4022, Oct. 1990.
7. Nallasamy, M and Groeneweg J.F., "Unsteady Blade surface Pressures on a Large-Scale Advanced Propeller: Prediction and Data," AIAA Paper 90-2402, July 1990.
8. Korkan, K.D., von Lavante, E. and Bober, L.J., "Numerical Evaluation of Propeller Noise Including Nonlinear Effects," AIAA Journal, Vol. 24, Jun. 1986, pp. 1043-1045.
9. Whitfield, C.E., Gliebe, P.R., Mani, R., and Mungur, P., "High Speed Turboprop Aeroacoustic Study(Single Rotation)," NASA-CR-182257, May 1989.
10. Hanson, D.B., "Near Field Frequency Domain Theory for Propeller Noise," AIAA Journal, vol. 23, April 1985, pp. 499-504.
11. Hanson, D.B., "Unified Aeroacoustics Analysis for Highspeed Turboprop Aerodynamics and Noise. Vol. I : Development of Theory for Blade Loading, Wakes and noise", NASA-CR-4329, to be published.
12. Ffowcs Williams J.E. and D.L. Hawkings, "Sound Generation by Turbulence and Surfaces in Arbitrary Motion," Philosophical Transactions of the Royal Society of London, Series A, Vol. 264, May 8, 1969, pp. 321-342.
13. Mani, R., "The Radiation of Sound From a Propeller at Angle of Attack," NASA-CR-4264, January 1990.
14. Envia, E., "Frequency Domain Analysis of Propfan Noise: A Moving Medium Formulation," NASA-CR to be published.
15. Wiener, F.M., "Sound Diffraction by Rigid Spheres and Circular Cylinders," Journal of the Acoustical Society of America, Vol. 19, No. 3, May 1947, pp. 444-451.
16. Dittmar, J.H., "Comparison of Propeller Cruise Noise Data Taken in the NASA Lewis 8- by 6-Foot Wind Tunnel with Other Tunnel and Flight Data," AIAA-89-1059, April 1989.
17. Lockheed Aeronautical Systems Company, "Propfan Test Assessment Flight Test Results Review," NAS3-24339 (DRD 235-03), NASA Lewis Research Center, November 14, 1988.
18. Woodward, R.P., "Measured Noise of a Scale Model High Speed Propeller at Simulated Take-off/Approach Conditions," AIAA paper 87-0526; also NASA-TM 88920.
19. Block, P.J.W., "The Effects of Installation on Single and Counter rotation Noise," AIAA Paper 84-2263, 1984.

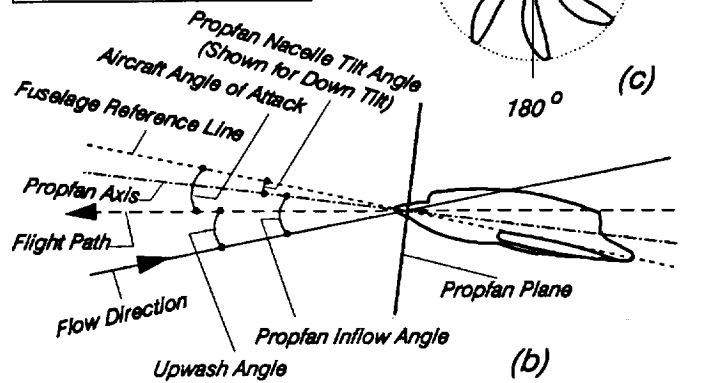


ORIGINAL PAGE  
BLACK AND WHITE PHOTOGRAPH



(a)

Propfan Inflow Angle =  
Aircraft Angle of Attack +  
Upwash Angle +  
Propfan Nacelle Tilt Angle



(b)

Fig. 1 SR7L propeller installed on the testbed aircraft.

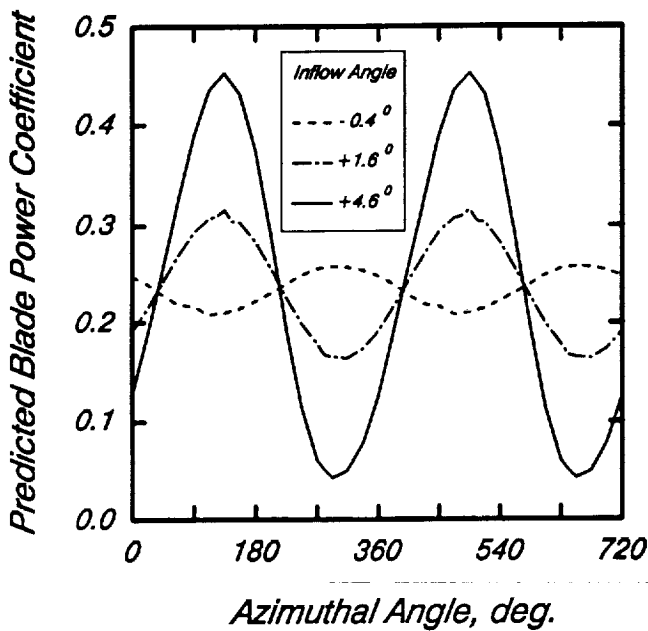


Fig. 2 Variation of per blade loading with azimuth angle

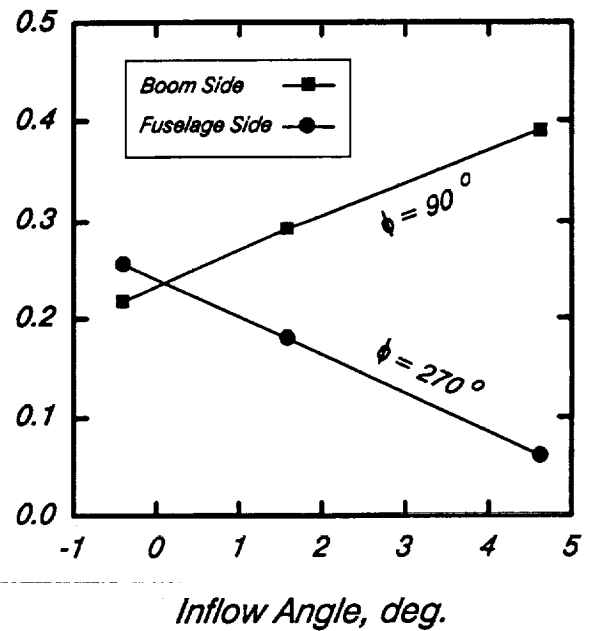


Fig. 3 Computed blade power variation with inflow angle.

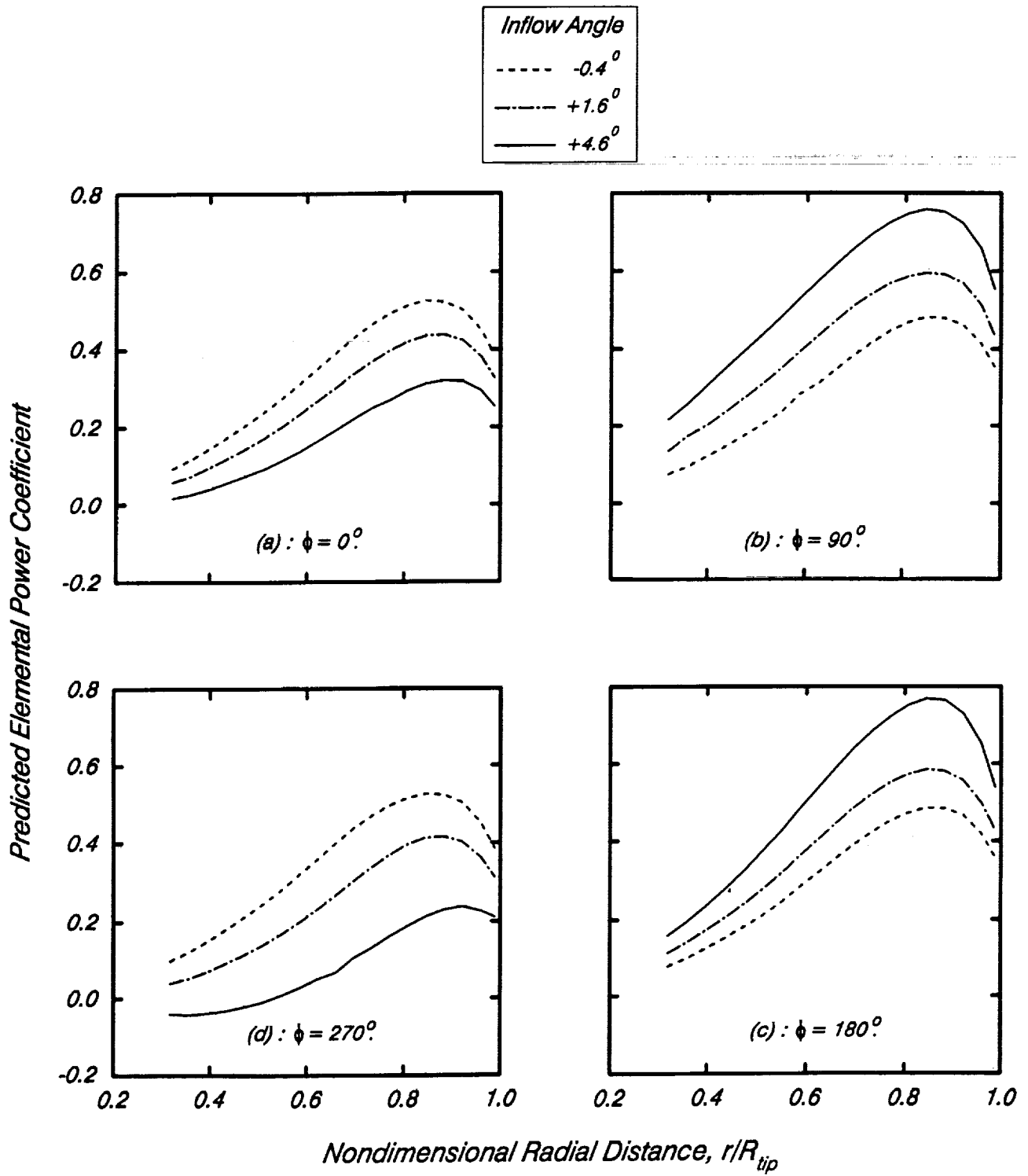
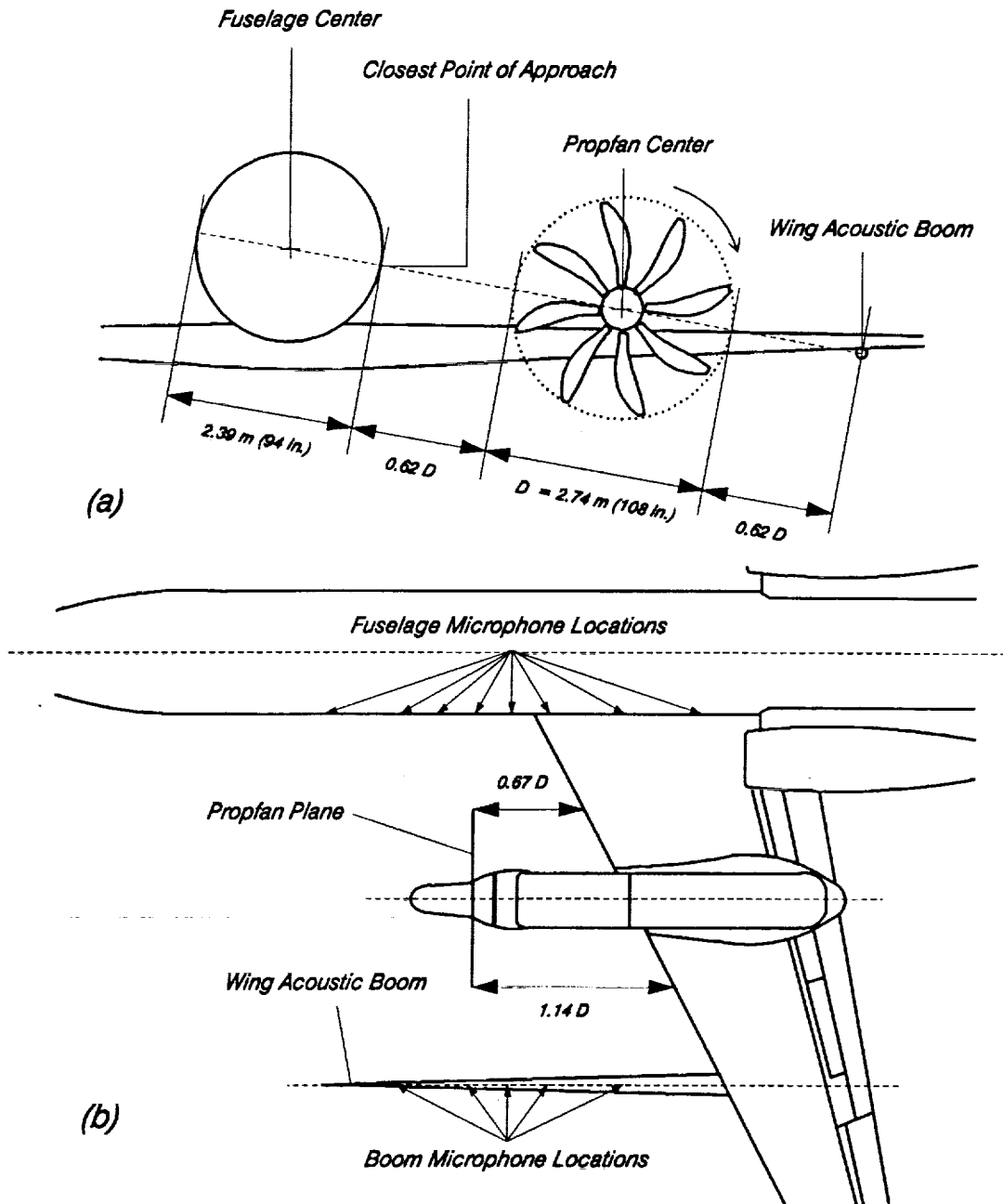


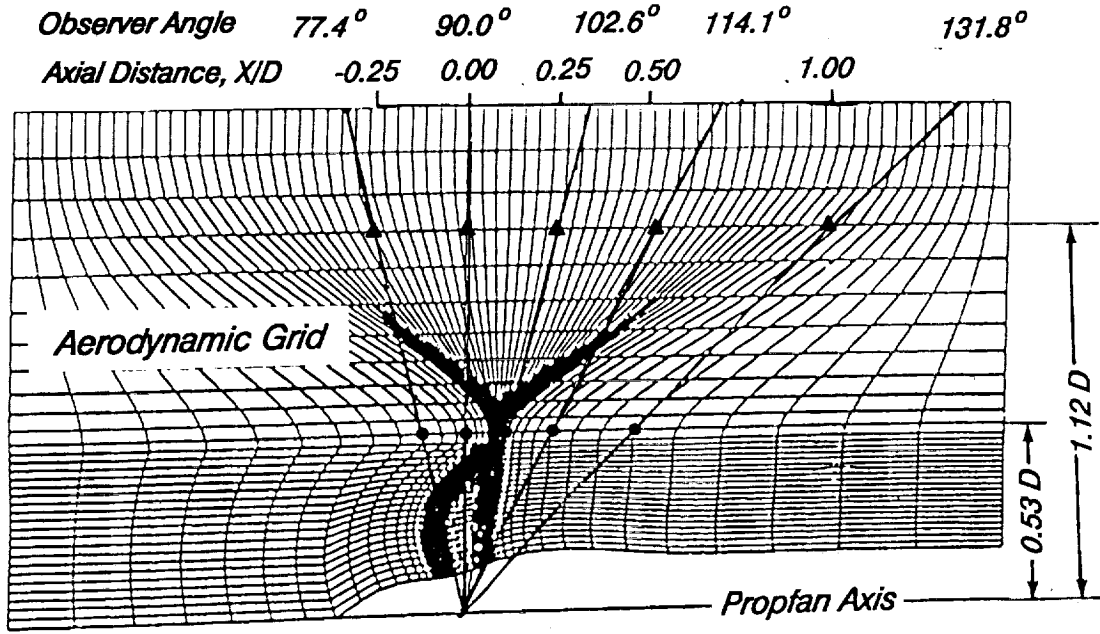
Fig. 4 Effect of inflow angle on elemental power coefficient variations.





	<i>Forward Locations</i>			<i>Propfan Plane</i>	<i>Aft Locations</i>			
<i>Axial Distance From Propfan Plane, X/D</i>	-1.00	-0.50	-0.25	0.00	0.25	0.50	1.00	1.50
<i>Boom Microphones</i>		•		•	•	•	•	
<i>Fuselage Microphones</i>	•	•	•	•	•	•	•	•

Fig. 6 PTA aircraft microphone locations selected for predictions.



*Sideline Microphone Locations* ▲

*Points Selected for Computation* ●

Fig. 7 Computational grid, axial-radial surface and points at which SPLs are computed in DCP.

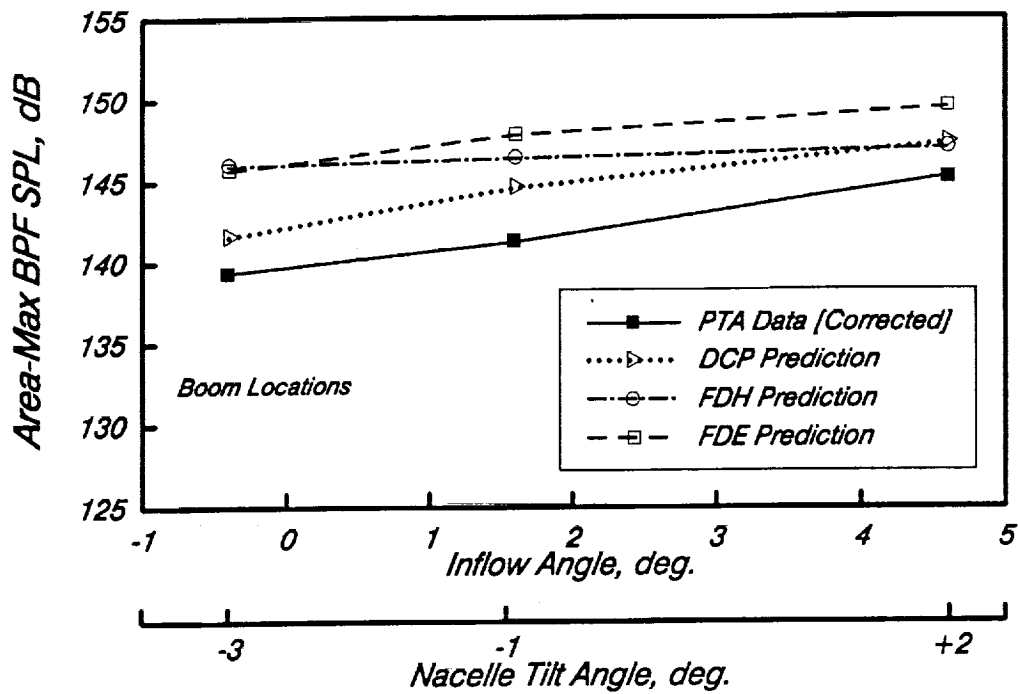


Fig. 8 Effect of inflow angle on the area-maximum BPF tone SPL at the boom microphone 1.12D sideline.

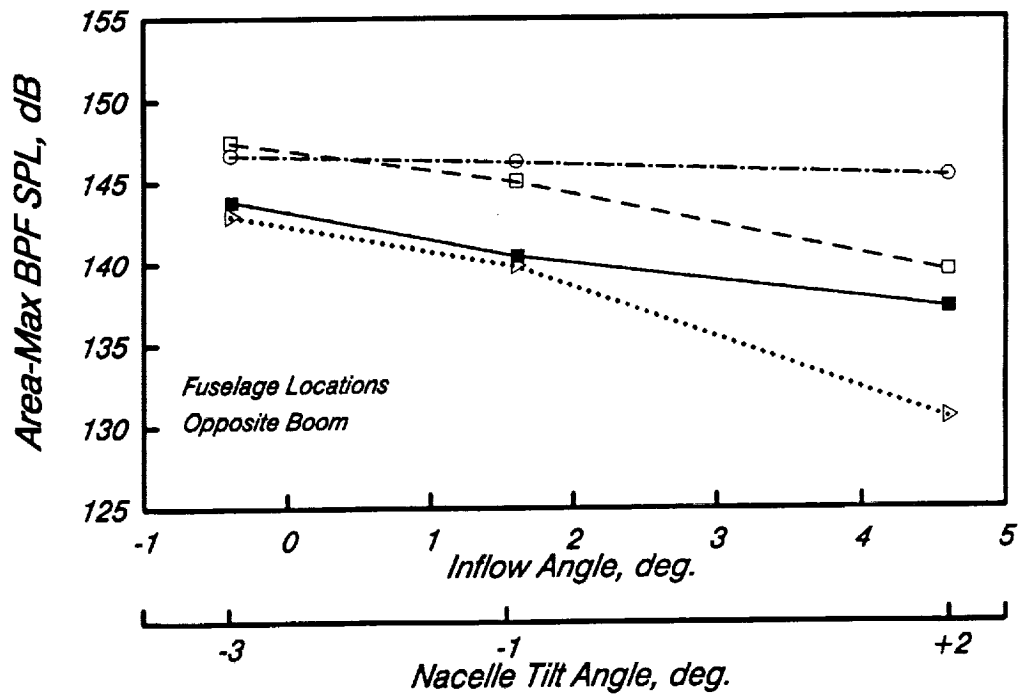


Fig. 9 Effect of inflow angle on the area-maximum BPF tone SPL at the fuselage microphone 1.12D sideline, opposite boom.

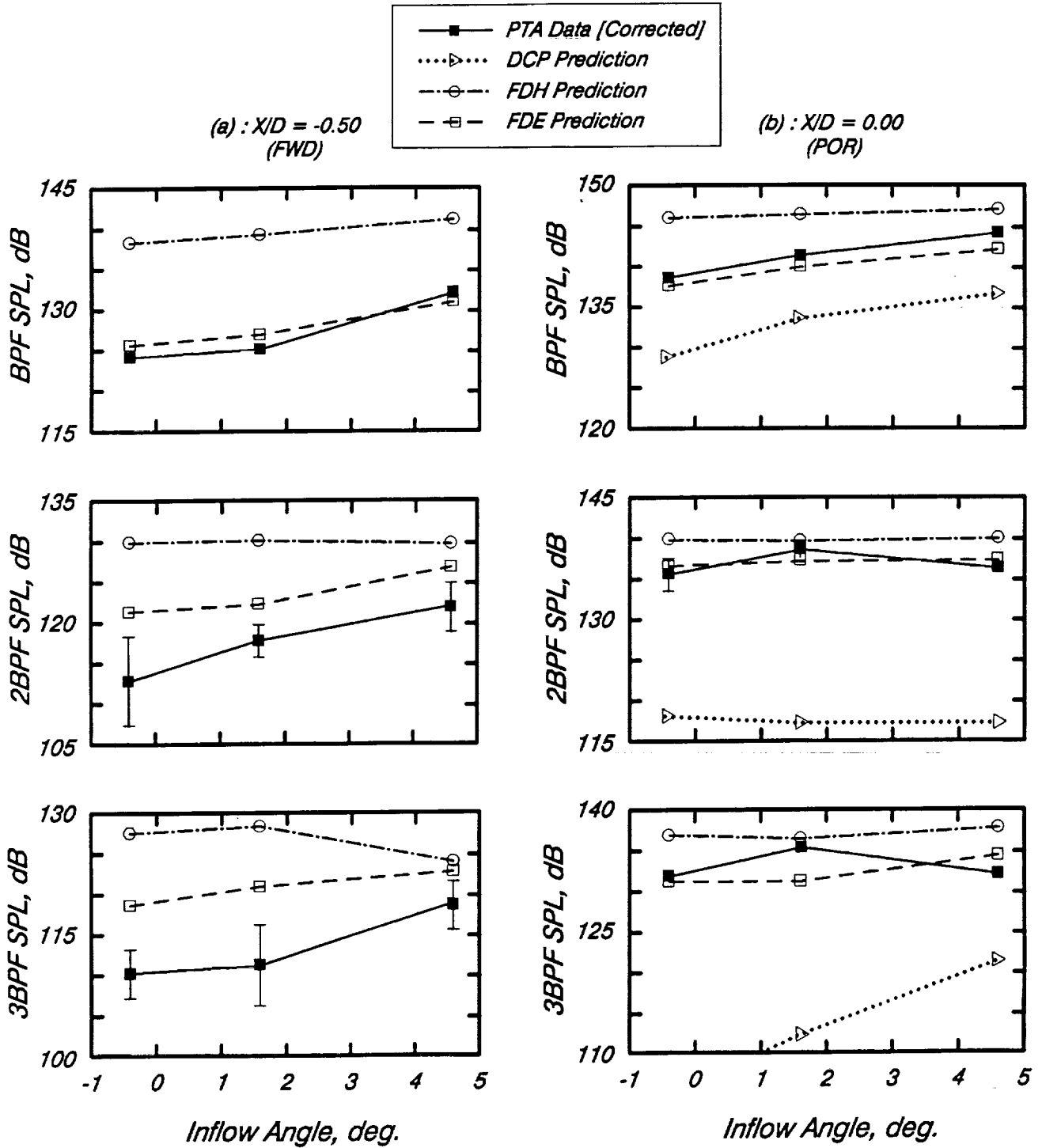


Fig. 10 Effect of inflow angle on the boom microphone SPLs for first three harmonics.

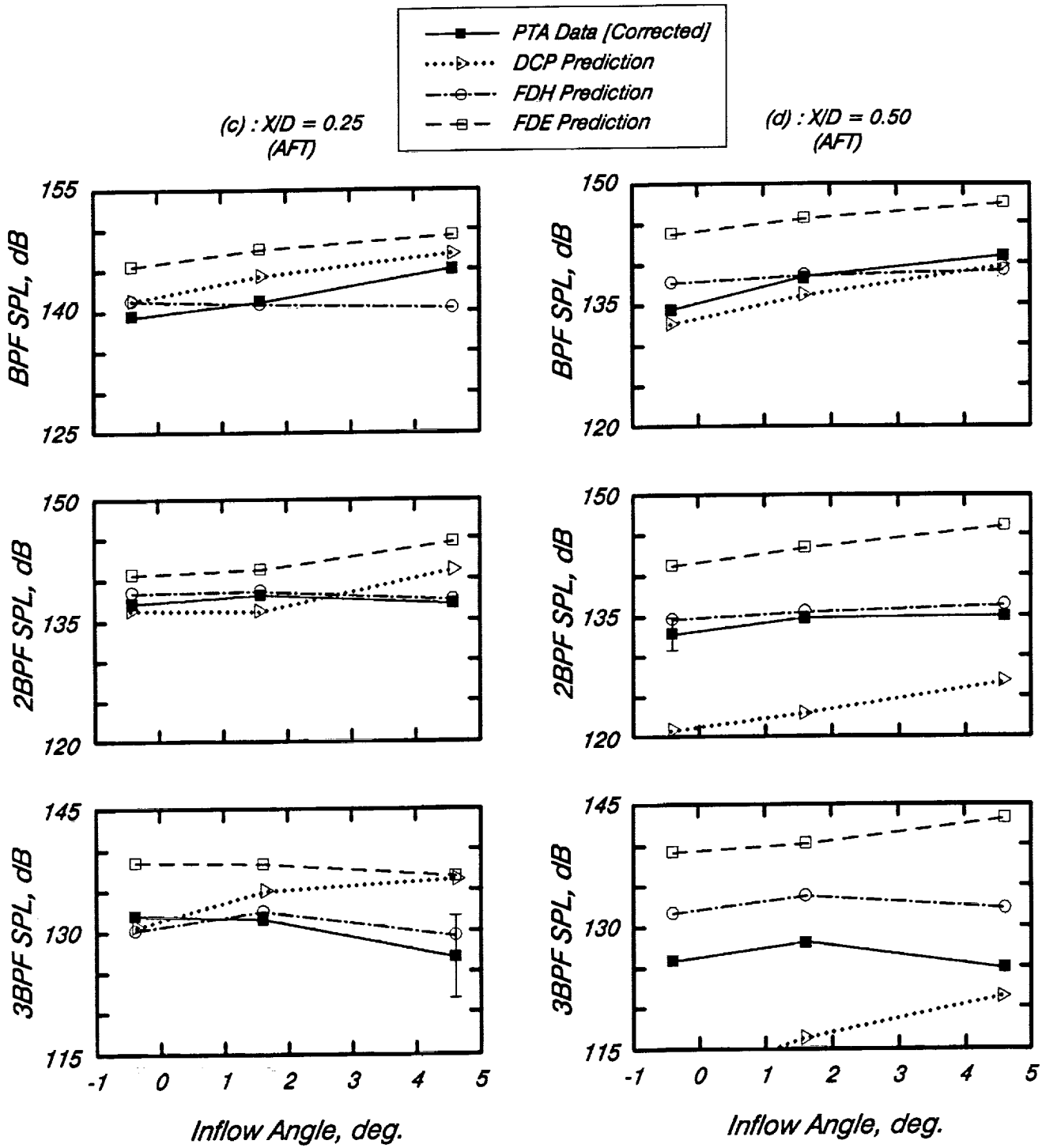


Fig. 10 Continued.



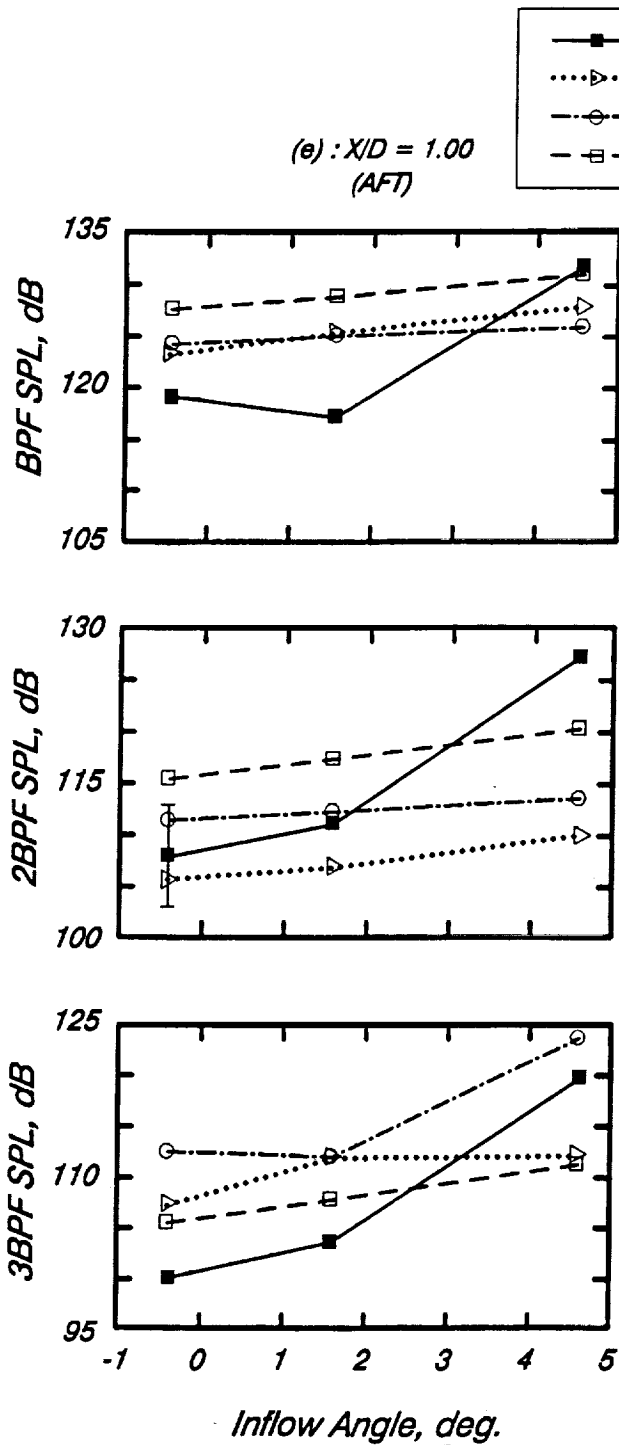


Fig. 10 Concluded.

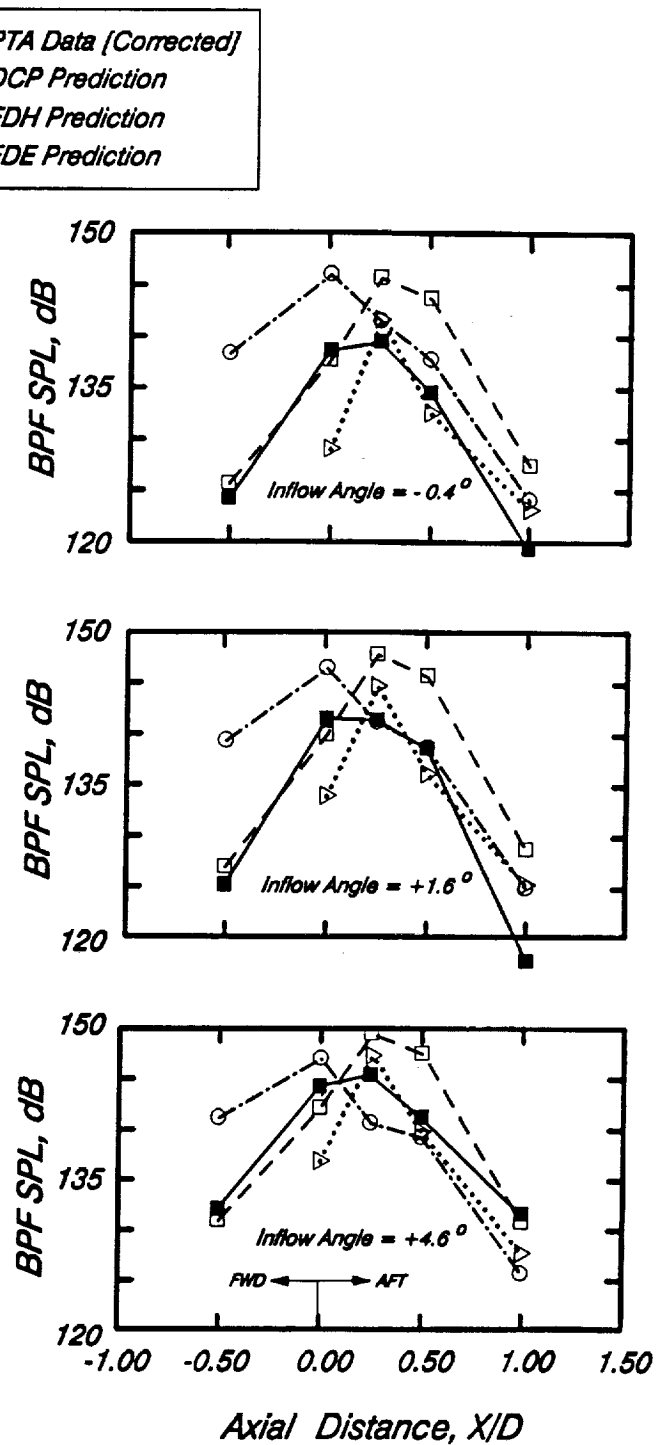


Fig. 11 1.12D sideline directivity-boom locations.

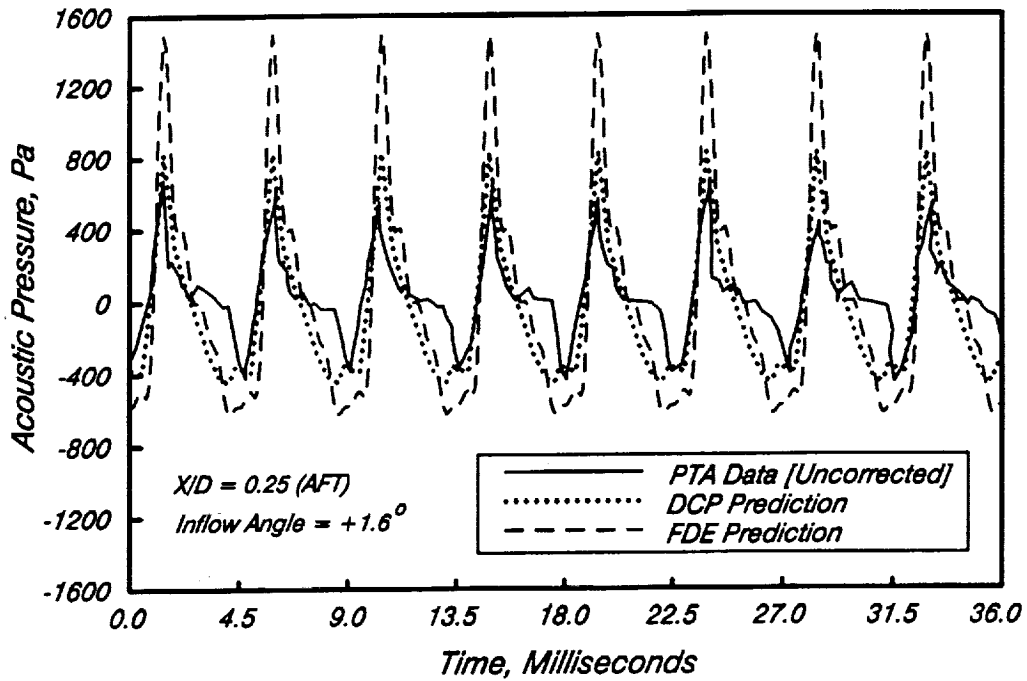


Fig. 12 Computed and measured sound pressure waveforms at 0.25D aft boom microphone location, inflow angle= $1.6^\circ$ .

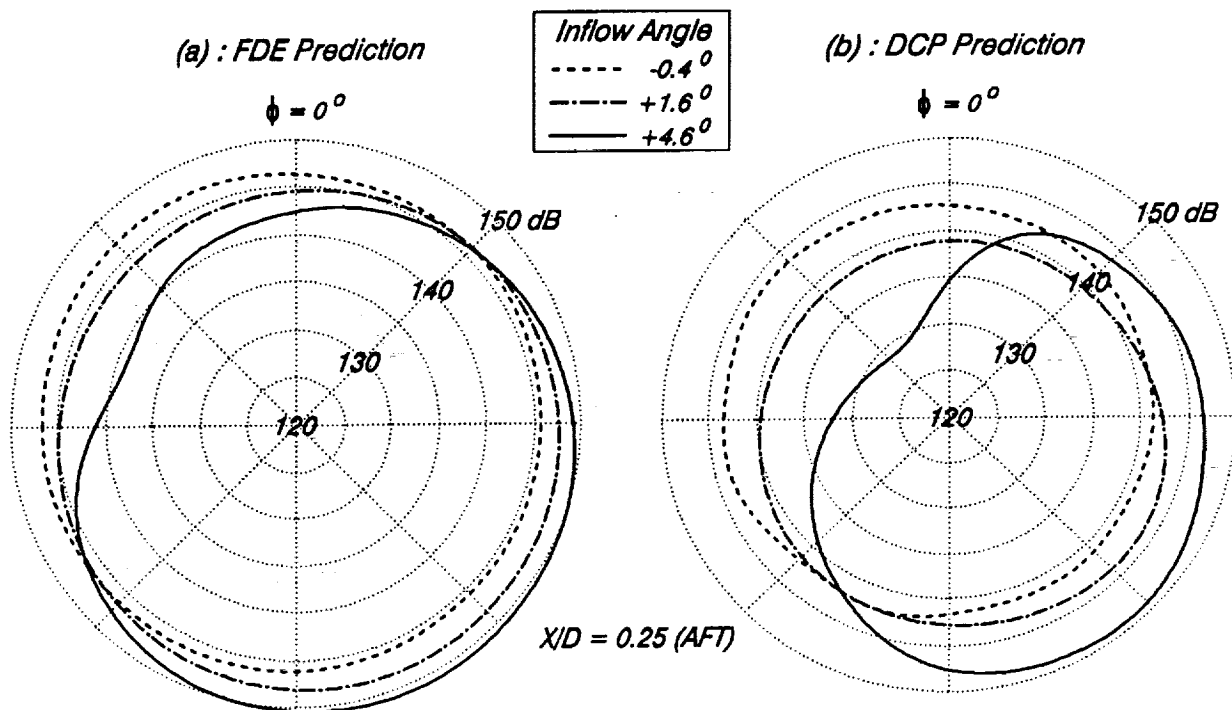


Fig. 13 Computed azimuthal directivity 0.25D aft.  
(a) FDE and (b) DCP predictions.

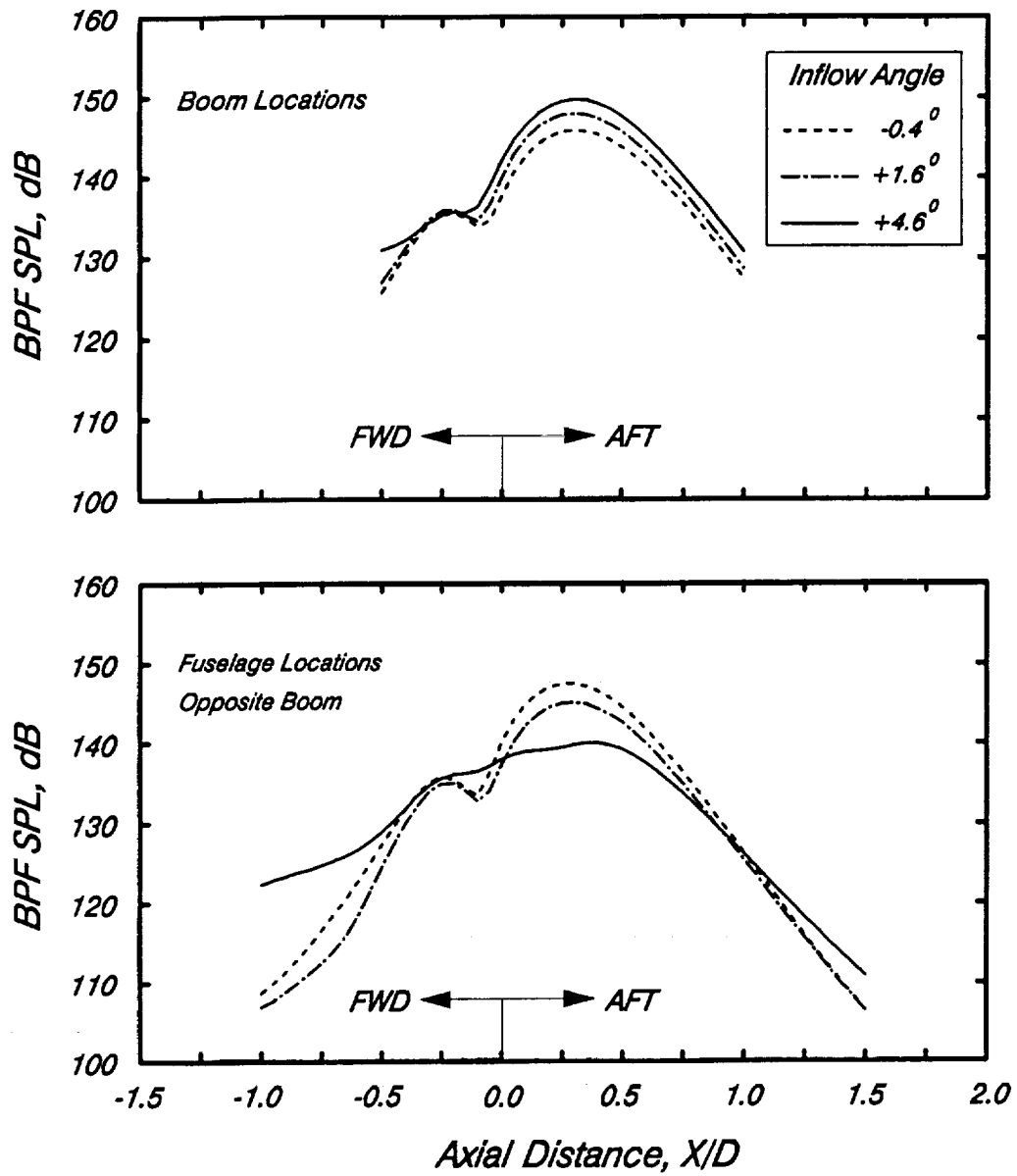


Fig. 14 1.12D sideline directivities at the boom microphone locations and fuselage locations opposite boom, FDE predictions.



# Report Documentation Page

1. Report No. NASA TM-103645 AIAA-90-3953		2. Government Accession No.		3. Recipient's Catalog No.	
4. Title and Subtitle Near-Field Noise of a Single-Rotation Propfan at an Angle of Attack				5. Report Date	
				6. Performing Organization Code	
7. Author(s) M. Nallasamy, E. Envia, B.J. Clark, and J.F. Groeneweg				8. Performing Organization Report No. E-5805	
				10. Work Unit No. 505-62-4D	
9. Performing Organization Name and Address National Aeronautics and Space Administration Lewis Research Center Cleveland, Ohio 44135-3191				11. Contract or Grant No.	
				13. Type of Report and Period Covered Technical Memorandum	
12. Sponsoring Agency Name and Address National Aeronautics and Space Administration Washington, D.C. 20546-0001				14. Sponsoring Agency Code	
				15. Supplementary Notes Prepared for the 13th Aeroacoustics Conference sponsored by the American Institute of Aeronautics and Astronautics, Tallahassee, Florida, October 22-24, 1990. M. Nallasamy and E. Envia, Sverdrup Technology, Inc., Lewis Research Center Group, 2001 Aerospace Parkway, Brook Park, Ohio 44142. B.J. Clark and J.F. Groeneweg, NASA Lewis Research Center.	
16. Abstract The near-field noise characteristics of a propfan operating at an angle of attack are examined utilizing the unsteady pressure field obtained from a three-dimensional Euler simulation of the propfan flowfield. The near-field noise is calculated employing three different procedures: a direct computation method in which the noise field is extracted directly from the Euler solution, and two acoustic-analogy-based frequency domain methods which utilize the computed unsteady pressure distribution on the propfan blades as the source term. The inflow angles considered are -0.4, 1.6, and 4.6 degrees. The results of the direct computation method and one of the frequency domain methods show qualitative agreement with measurements. They show that an increase in the inflow angle is accompanied by an increase in the sound pressure level at the outboard wing boom locations and a decrease in the sound pressure level at the (inboard) fuselage locations. The trends in the computed azimuthal directivities of the noise field also conform to the measured and expected results.					
17. Key Words (Suggested by Author(s)) Turboprops Unsteady Euler solutions Unsteady pressures Acoustics			18. Distribution Statement Unclassified - Unlimited Subject Category 71		
19. Security Classif. (of this report) Unclassified		20. Security Classif. (of this page) Unclassified		21. No. of pages 18	22. Price* A03